INVITED SURVEY PAPER

Evolution Trends of Wireless MIMO Channel Modeling towards IMT-Advanced

Chia-Chin CHONG[†a)], **Fujio WATANABE**[†], *Nonmembers*, **Koshiro KITAO**[††], **Tetsuro IMAI**[††], *and* **Hiroshi INAMURA**[†], *Members*

SUMMARY This paper describes an evolution and standardization trends of the wireless channel modeling activities towards IMT-Advanced. After a background survey on various channel modeling approaches is introduced, two well-known multiple-input-multiple-output (MIMO) channel models for cellular systems, namely, the 3GPP/3GPP2 Spatial Channel Model (SCM) and the IMT-Advanced MIMO Channel Model (IMT-Adv MCM) are compared, and their main similarities are pointed out. The performance of MIMO systems is greatly influenced by the spatial-temporal correlation properties of the underlying MIMO channels. Here, we investigate the spatial-temporal correlation characteristics of the 3GPP/3GPP2 SCM and the IMT-Adv MCM in term of their spatial multiplexing and spatial diversity gains. The main goals of this paper are to summarize the current state of the art, as well as to point out the gaps in the wireless channel modeling works, and thus hopefully to stimulate research in these areas.

key words: *channel model, IMT-Advanced, MIMO, multipath, spatial diversity, spatial multiplexing*

1. Introduction

Accurate knowledge of the wireless propagation channel is of great importance when designing radio systems. A realistic radio channel model that provides insight into the radio wave propagation mechanisms is essential for the design and successful deployment of wireless systems. Unfortunately, the mechanisms that govern radio propagation in a wireless communication channel are complex and diverse. Therefore, a better understanding of the propagation mechanisms is key towards the development of a realistic channel model. Consequently, channel modeling has been a subject of intense research for a long time [1]–[5].

Standard channel models are essential for the development of new radio systems and technology. These models if implemented as channel simulators allow the performance evaluation of different transmission technologies, signal processing techniques and receiver (RX) algorithms through computer simulations. Therefore, this can avoid the necessity to build hardware prototype or to perform field-trials for every configuration to be considered. Generally speaking, if accurate channel models are available, it is possible to design transmission technologies and RX algorithms that can achieve good performance by exploiting the properties of the propagation channel. While the channel models should be accurate enough in order to capture sufficient properties from the real propagation effect, these models should also be simple enough to allow feasible implementation and reasonable short simulation times. Therefore, a tradeoff between "accuracy" and "simplicity" should be taken into consideration when developing a good channel model depending on the type of system to be evaluated.

The type of channel model that is desired depends critically on the carrier frequency, bandwidth, the type of environment and system under consideration. For example, different types of channel models are needed for indoor and outdoor environments, and for narrowband, wideband and ultrawideband systems. Early channel modeling work aimed to develop models which could provide an accurate estimate of the mean received power and to study the behavior of the received signal envelope. This lead to pathloss models such as the Okumura-Hata model [6], Lee's model [7], COST* 231 Walfish-Ikegami model [8]–[10] and the conventional statistical models for the fading signal envelope [2], [4], [5]. Since these models were typically developed for narrowband systems, the temporal domain such as delay spread for the power delay profile (PDP) was largely neglected. As the need for higher data rates increased, larger bandwidths became necessary. In order to accurately model wideband systems, narrowband channel models were enhanced to include the prediction of the temporal domain properties such as the delay spread of the PDP. The COST 207 model [11], which was used in the evaluation of the Global System for Mobile Communication (GSM) systems, as well as the ITU-R** IMT-2000*** model [12] are examples of such wideband channel models. Due to the evolution of analog to digital wideband systems, these models were important when analyzing digital modulation over wireless communication links and for cell planning in digital mobile radio for second generation (2G) systems.

In the third generation (3G) and Beyond 3G (B3G)/fourth generation (4G) cellular systems, higher data rate transmissions and better quality of services are demanded in order to improve user experience. This motivates the investigation of how efficiently the available ra-

Manuscript received September 8, 2008.
Manuscript revised January 27, 2009.

[†]The authors are with the Wireless Access Laboratory, DOCOMO Communications Laboratories USA, Inc., USA.
[††]The authors are with the Radio Access Network Development Department, NTT DOCOMO, Inc., Yokosuka-shi, 239-8536 Japan.
a) E-mail: cchong@docomolabs-usa.com
DOI: 10.1587/transcom.E92.B.2773

*Cooperation in Science and Technology.
**International Telecommunications Union Radiocommunication Sector.
***International Mobile Telecommunications-2000.

dio channel resources should be utilized in order to fully exploit the time, frequency, and spatial domains. Smart antennas exploit the spatial behavior of the mobile radio channel and have been one of the key technologies towards the successful introduction of 3G systems such as Universal Mobile Telecommunication System (UMTS) and CDMA2000. In order to exploit the spatial dimension efficiently, it is essential to have a profound knowledge of the spatial-temporal propagation characteristics between a base station (BS) and a mobile station (MS). However, in most initial 3G systems such as Wideband Code Division Multiple Access (WCDMA) Rel-99, High-Speed Downlink Packet Access (HSDPA), High-Speed Uplink Packet Access (HSUPA), CDMA2000 HRPD† Rel-0, HRPD Rev-A and HRPD Rev-B, smart antennas were mainly deployed at the BS only. Therefore, at that time, most spatial channel models available in the open literature only incorporated directional information at the BS side [13]–[17].

The B3G and 4G cellular systems such as Evolved High-Speed Packet Access (HSPA+), Long Term Evolution (LTE), LTE-Advanced, Ultra Mobile Broadband (UMB) (a.k.a. HRPD Rev-C), and Mobile WiMAX (e.g., IEEE 802.16e, IEEE 802.16 m) all exploit spatial information at both BS and MS. These systems deploy multiple-input-multiple-output (MIMO) technology whereby multiple antenna elements are being used at both ends of the transmission link. MIMO has emerged as one of the most promising breakthroughs in wireless communications due to its capability of improving link reliability and to significantly increase the link capacity [18]–[21] as long as the channel provides sufficient scattering. Such advantages can enhance the network's quality of service and increase the operator's revenues due to higher spectral efficiency and throughput. However, the actual performance of the MIMO systems is very much influenced by the wireless channel under consideration. For instance, the degree of spatial correlation among the antenna elements, the local scattering angular spread, the rank of the MIMO channel, etc. are some of the important limiting factors for the achievable capacity and diversity gains. Therefore, appropriate characterization and modeling of MIMO propagation channels are essential for designing MIMO transceiver and evaluating MIMO performance.

The concept of the *double-directional channel* was first introduced in [22] and since then, many channel measurement and modeling works based on this concept were reported in the literature [23]–[31]. Such a model is useful for MIMO systems since it includes angular information at both the BS and the MS, and it is more well-known among the industrials as simply *MIMO channel*. The standardization of MIMO channel models were reported in 3GPP and 3GPP2 (i.e., 3GPP/3GPP2 Spatial Channel Model (SCM) [32]), WiMAX Forum (i.e., Mobile WiMAX MIMO Channel Model [33]), IEEE 802.11n (i.e., TGn Channel Models [34]), and ITU-R Working Party 5D (WP5D) (i.e., IMT-Advanced MIMO Channel Model (IMT-Adv MCM) [35]) for cellular, mobile broadband wireless access, wireless local area networks (WLANs) and IMT-Advanced systems, respectively. The main focus of this paper are the standardized MIMO channel models used in both 3G and B3G/4G cellular systems, namely, the 3GPP/3GPP2 SCM and the IMT-Adv MCM. Other standardized models designed for single-input-multiple-output (SIMO) or single-input-single-output (SISO) channels will not be discussed here.

The paper is organized as follows. Section 2 establishes the fundamental concepts and background for various channel modeling approaches; Sect. 3 discusses the two well-known standard MIMO channel models, namely, the 3GPP/3GPP2 SCM and the IMT-Adv MCM, used in 3G and B3G/4G cellular systems; Sect. 4 compares these two MIMO channel models in term of their spatial multiplexing and spatial diversity gains; finally, in Sect. 5 appropriate conclusions are drawn.

2. Channel Modeling Approach

The requirement to model many different types of wireless propagation channels has resulted in a large number of different modeling approaches reported in the literature [36]–[38]. One reason for the abundance of modeling approaches is due to the complex phenomena encountered by a transmitted signal. The transmitted signal will usually arrive at the RX via several paths, i.e., multipaths, where the signal encounters various propagation mechanisms such as reflection, scattering and/or diffraction. Figure 1 illustrates a typical wireless channel in outdoor environment whereby, a signal transmitted by the BS is reflected by several objects within the channel before reaching the MS. Therefore, many different types of simplifications and approximations are necessary in order to obtain a simple yet accurate and reliable model of the wireless communications channel. According to [39], propagation channel models can be broadly divided into two main categories, namely, *deterministic approach* and *stochastic approach* (or *statistical approach*). In general, these models differ in terms of their usage and the type of underlying data. Under each category, channel models can be further grouped according to the method by which they were developed as summarized in Fig. 2. In this section, some existing channel models in each category are referred. The list is not meant to be exhaustive, but merely serve as a stepping-stone towards the discussion in the rest of the paper.

2.1 Deterministic Approach

There are three different subcategories of deterministic approach, namely, *closed-form approach*, *measurement-based approach* and *ray-tracing approach*. Deterministic models may exist in closed-form for very simple channels such as a two-path signal model. Such models are usually too restrictive to represent any realistic communication environment. Direct measurement of the channel impulse response provides an empirical model for the measured scenarios. The

†High Rate Packet Data.

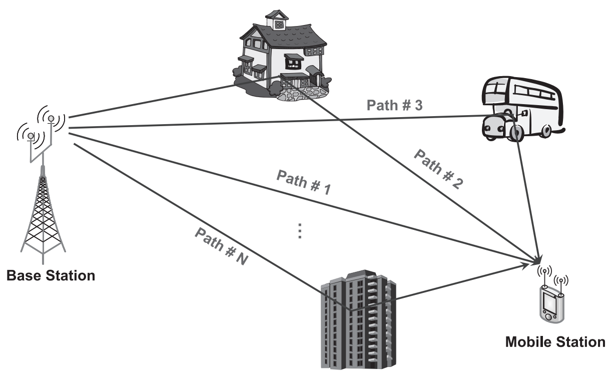

Fig. 1 Illustration of a typical wireless channel in outdoor environment.

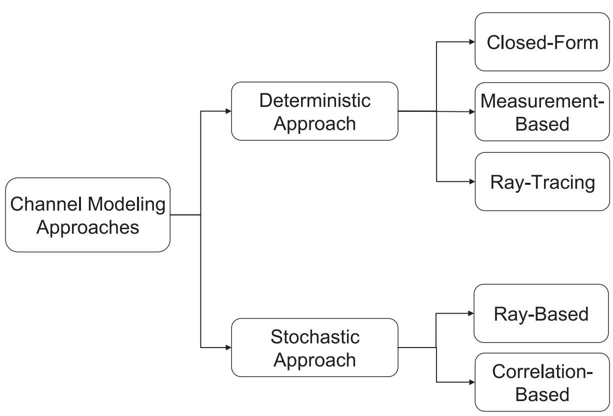

Fig. 2 Classification of channel modeling approaches.

data is usually collected with channel sounders by transmitting known signals and comparing them with the received signals. The main advantage of such an approach is that the measured channel responses are usually very accurate. However, the downside is that the measured data is very site-specific and therefore, characterization of all types of channels by measurement becomes a non-trivial task due to the requirement of vast amount of data. Furthermore, channel measurements are very costly, which limits the amount of data that can be collected. A number of measurement-based deterministic channel models have been developed and reported in the literature [40], [41].

Ray-tracing approach apply an electromagnetic simulation tool such as ray launching and imaging methods to obtain nearly exact propagation characteristics for a specified geometry. Firstly, a site-specific environment is generated from a detailed map, in which the BSs and MSs are placed. Then, based on the known transmitting signals these models describe the physics of the propagation mechanisms (e.g., reflection, diffraction and scattering) in order to calculate the received signals. Note that, these calculations require a far-field assumption to be feasible. The accuracy of the models rely on the accuracy and detail of the site-specific propagation medium [42]. Therefore, this approach should be employed only when detailed environment data is available such as the position, size and orientation of man-made objects (e.g., buildings, bridges, roads, etc.) as well as natural objects (e.g., trees, mountains, etc.). The basic idea behind the ray-tracing approach is that, if the propagation environment is known to a sufficient degree, wireless propagation is a deterministic process that allows determining its characteristics at every point in space. Typically, the ray-tracing approach is used for cell and network planning. The major advantage of ray-tracing models is that they offer great accuracy with site-specific results. Ideally, any site can be modeled if its physical characteristics are available, and any channel parameter can be calculated by adjusting these models. However, in reality these physical parameters are either unavailable or cannot be perfectly obtained. This subsequently could lead to degradation in the accuracy of the ray-tracing model. Furthermore, these models have several disadvantages. Firstly, the topographical and environment data is always tied to a particular site and thus, a huge amount of such data is required in order to obtain a comprehensive set of different propagation environments. Secondly, they are usually computationally expensive, especially when the environment is complex. Thus, detailed physical characteristics of the simulated environment must be known beforehand which is often time-consuming and impractical. Numerous ray-tracing models for cellular networks have been reported in the literature such as [43]–[53] and the references therein.

2.2 Stochastic Approach

Stochastic models are normally less complex than the deterministic models, and can provide sufficiently accurate channel information. These models attempt to generate synthetic channel responses that are representative of real propagation channels. Firstly, measurements will be conducted in a large variety of locations and environments in order to obtain a database with good representation of the underlying statistical properties. Then, the probability density function (pdf) of the channel parameters will be derived from the measurement data which will be used to regenerate the channel impulse responses. Since the stochastic approach is based on probabilistic characterization of the wireless channel, models based on this approach can be tuned to imitate various propagation environments by setting appropriate values for the channel parameters. Note that fixed parameter settings do not produce identical outputs on each simulation run but stochastic processes are used to create variability within a fixed environment type. For example, a particular set of parameters might generate a representative set of propagation scenarios found in outdoor urban environments. Many channel models have been developed under this category for cellular systems design and cell planning such as the Okumura-Hata pathloss model [6], the widely used COST 207 model [11], its successors UMTS Code Division Testbed (CODIT) model [54] and Advanced Time Division Multiple Access (ATDMA) model [55].

In general, stochastic approach can be classified into two main subcategories, namely, *ray-based approach* (a.k.a.

geometrically-based stochastic approach) and *correlation-based approach*. The ray-based modeling approach is commonly used in MIMO channel modeling. This approach assumes that a number of scatterers is distributed in space according to some stochastic distribution around the transmitter (TX) and RX ends. The channel gains are then calculated for each antenna at both TX and RX ends by summing the contribution from each reflected ray emerging from the scatterer. Multiple rays, each with its own amplitude, angle-of-departure (AoD), angle-of-arrival (AoA), time-of-arrival (ToA), and phase, add constructively and destructively, whereby the received signal can be modeled as a superposition of rays. The summed received signal can then be written as

$$h(t) = \sum_{n=1}^{N} \alpha_n \exp\left(j2\pi f_n t + \phi_n\right), \tag{1}$$

where α_n is the amplitude, f_n is the frequency, and ϕ_n is the phase of the n-th ray. Within this subcategory, the widely deployed models are the 3GPP/3GPP2 SCM [32] and the IMT-Adv MCM [35] for 3G and B3G/4G cellular systems, respectively. Other examples of ray-based models are such as [56]–[61].

The correlation-based modeling approach relies on the channel second order statistics such as correlation and covariance matrices. In particular, this approach models the transfer function of each transmit and receive antenna element pair, and the signal correlations between them. The generation of MIMO channel matrices based on channel correlation matrix is defined as

$$\mathbf{R} = \mathbb{E}\left[\mathrm{vec}\left(\mathbf{H}\right)^{\mathcal{H}} \mathrm{vec}\left(\mathbf{H}\right)\right], \tag{2}$$

where $\mathbb{E}[\cdot]$ denotes the expectation, $(\cdot)^{\mathcal{H}}$ denotes the Hermitian transpose, $\mathrm{vec}(\cdot)$ is the vectorization operator, and $\mathbf{H}$ is the MIMO channel matrix. In order to simplify the analysis, one example of such a model is the Kronecker model in which the channel correlation matrix $\mathbf{R}$ can be written as follows

$$\mathbf{R} = \mathbf{R}_{\mathrm{Tx}} \otimes \mathbf{R}_{\mathrm{Rx}}, \tag{3}$$

where $\otimes$ is the Kronecker product and $\mathbf{R}_{\mathrm{Tx}}$ and $\mathbf{R}_{\mathrm{Rx}}$ are the correlation matrices at the TX and RX, respectively. The advantage of the Kronecker assumption is that (3) is a computationally simpler operation than the full correlation matrix in (2). The underlying assumption is that the directional properties of the channel at the TX and RX are independent.

Both ray-based and correlation-based stochastic channel models have advantages and disadvantages. For instance, the ray-based channel models can directly generate channel coefficients, in which the spatial-temporal correlation is implicitly present in the channel matrix generation. However, since it does not specify the spatial-temporal correlation properties explicitly, it is therefore difficult to connect its simulation results with the theoretical analysis. Furthermore, the implementation complexity of the ray-based models are usually high since many parameters have to be generated such as antenna array orientations, mobile directions, delay spread, angular spread, AoDs, AoAs, and phases. On the other hand, for the correlation-based models, the spatial correlation is explicitly defined and generated by means of spatial correlation matrices. This provides elegant and concise analytical expressions for the MIMO channel and makes the correlation-based models easier to be integrated into a theoretical framework. The main advantage of the correlation-based approach are its computational and modeling simplicity whereby it requires less input parameters as compared to the ray-based approach. However, despite its simplicity and analytical tractability, the correlation-based model is restricted to model only the average spatial-temporal behavior of the MIMO channels. There are several other drawbacks of the correlation-based approach. For instance, the correlation matrix is antenna array dependent and hence has to be re-estimated for different array geometries. Also, the model parameterization describes only the second-order statistics of the channel without any physical interpretation of the propagation medium. In particular, with the Kronecker assumption, the correlation-based models are deemed to over simplify the MIMO channel characteristics since they are incapable of reproducing the "pinhole" [50] or "keyhole" [62], [63] effects which results in low rank (hence low capacity) channels. Due to the above reasons, the ray-based model is preferred as it provides more insights of the variations of different MIMO channel realizations. Figures 3 and 4 illustrate the ray-based and the correlation-based (Kronecker approach) MIMO channel models, respectively.

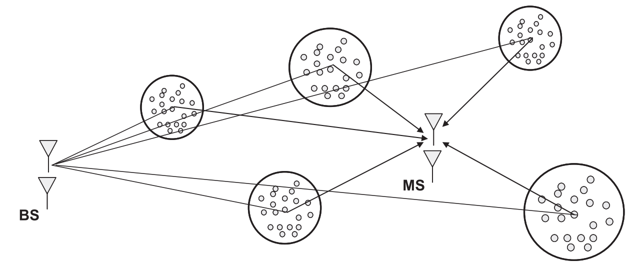

Fig. 3 Illustration of the ray-based MIMO channel model.

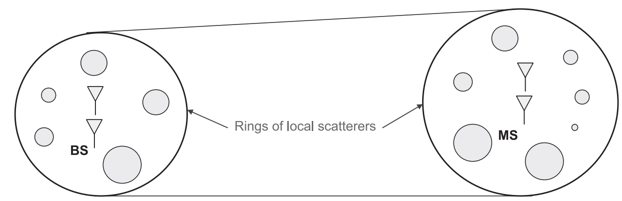

Fig. 4 Illustration of the correlation-based (Kronecker approach) MIMO channel model.

3. Standard MIMO Channel Models for 3G and B3G/4G Cellular Systems

In order to evaluate the performance of various air-interface

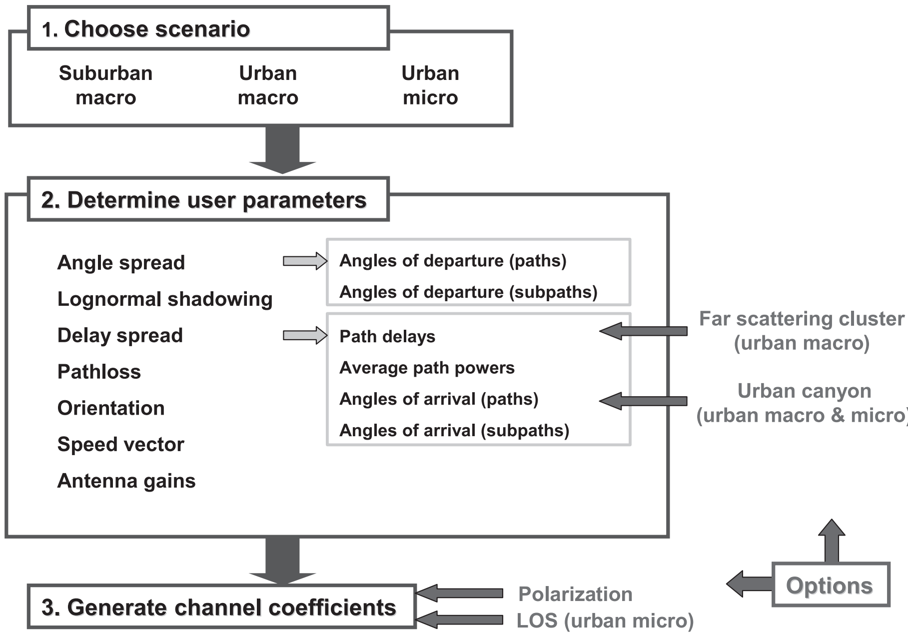

Fig. 5 The overview of the 3GPP/3GPP2 SCM channel coefficients generation procedure [32].

technologies based on MIMO schemes, several MIMO channel models have been developed in either standard organizations (e.g., 3GPP/3GPP2 SCM and IMT-Adv MCM) or within large collaborative projects (e.g., IST Multi Element Transmit and Receive Antennas (METRA) Channel Model [25], IST Wireless World Initiative New Radio (WINNER) model [64], COST 259 Directional Channel Model [29], and COST 273 MIMO Channel Model [65]). In this section, two MIMO channel models, i.e., the 3GPP/3GPP2 SCM and the IMT-Adv MCM suitable for system-level simulations will be reviewed and compared. Both models deploy the geometrically-based stochastic modeling approach as the channel model framework and can be applied for different environments (e.g., urban macro, urban micro, etc.). Each environment has specific distributions and parameters. By changing these specific distributions in angle and delay domains as well as the environment specific parameters, different channel models under different environments and scenarios (e.g., line-of-sight (LOS) and non-LOS (NLOS)) can be generated.

3.1 3GPP/3GPP2 Spatial Channel Model (SCM)

The SCM was developed within 3GPP/3GPP2 ad-hoc group as a reference model for evaluating different MIMO techniques. The model was first released in September 2003 [66] and was later updated in June 2007 [32]. It defines three most commonly used environments in cellular systems, namely, suburban macro, urban macro, and urban micro. For all these scenarios, the number of paths (a.k.a. clusters) are fixed to six and each path consists of 20 spatially separated subpaths (a.k.a. rays). The SCM was parameterized for systems with 5 MHz bandwidth and a center frequency around 2 GHz. Therefore, it is valid for most 3G systems deploying MIMO techniques and may not be suitable for system with bandwidth higher than 5 MHz. The SCM was later extended by [67] as the Spatial Channel Model Extension (SCME) which support up to 100 MHz bandwidth in order to evaluate the 3GPP LTE systems.

The overall procedure for generating the SCM channel coefficients can be summarized in three steps as illustrated in Fig. 5. Firstly, one of the three environments as described above will be chosen. After the number of BSs with their respective cell layouts (e.g., hexagonal layout) and inter-site distances have been determined, MSs are randomly positioned within each cell. Then, each of the MS will be given a random antenna array orientation drawn from a uniform $[0, 360°]$ distribution and a random velocity with its direction also drawn from a uniform $[0, 360°]$ distribution. Secondly, the channel parameters for the selected environment will be determined. This can be categorized into large-scale (LS) parameters such as delay spread (DS), angular spread (AS) and shadowing fading (SF); and small-scale (SS) parameters such as paths' powers, delays, AoAs and AoDs, as well as subpaths' AoAs and AoDs. Thirdly, the channel coefficients are generated. Based on the SCM, six paths are generated, each with a given angular dispersion power, AoA and AoD. This dispersion is due to the fact that there are 20 subpaths within each path, and each subpath has a slightly different AoA and/or AoD but with the same time delay. Here, the paths' powers, delays, and angular properties for both sides of the link are modeled as random variables (RVs) defined by pdfs and cross-correlations.

When generating channel coefficients using the SCM, a number of "drops" are generated. A "drop" is defined as a simulation run for a given number of cells/sectors, BSs, and MSs over a short period of time. During a drop, the channel undergoes fast-fading according to the motion of

Table 1 The 3GPP/3GPP2 SCM channel model parameters [32].

Channel Scenario	Suburban Macro	Urban Macro	Urban Micro
Number of paths, N	6	6	6
Number of subpaths per path, M	20	20	20
Mean AS at BS	$\mathbb{E}(\sigma_{AS,BS}) = 5°$	$\mathbb{E}(\sigma_{AS,BS}) = 8°, 15°$	NLOS: $\mathbb{E}(\sigma_{AS,BS}) = 19°$
AS at BS as a lognormal RV $\sigma_{AS} = 10^{(\epsilon_{AS} \cdot x + \mu_{AS})}$, where $x \sim N(0, 1)$	$\mu_{AS} = 0.69$ $\epsilon_{AS} = 0.13$	For $8°$, $\mu_{AS} = 0.81$ $\epsilon_{AS} = 0.34$ For $15°$, $\mu_{AS} = 1.18$ $\epsilon_{AS} = 0.21$	N/A
$r_{AS} = \sigma_{AoD}/\sigma_{AS}$	1.2	1.3	N/A
Per-path AS at BS (fixed)	2°	2°	5° (LOS and NLOS)
BS per-path AoD distribution standard deviation	$N(0, \sigma^2_{AoD})$, where $\sigma_{AoD} = r_{AS} \cdot \sigma_{AS}$	$N(0, \sigma^2_{AoD})$, where $\sigma_{AoD} = r_{AS} \cdot \sigma_{AS}$	$U(-40°, 40°)$
Mean AS at MS	$\mathbb{E}(\sigma_{AS,MS}) = 68°$	$\mathbb{E}(\sigma_{AS,MS}) = 68°$	$\mathbb{E}(\sigma_{AS,MS}) = 68°$
Per-path AS at MS (fixed)	35°	35°	35°
MS per-path AoA distribution	$N(0, \sigma^2_{AoA}(Pr))$	$N(0, \sigma^2_{AoA}(Pr))$	$N(0, \sigma^2_{AoA}(Pr))$
DS as a lognormal RV $\sigma_{DS} = 10^{(\epsilon_{DS} \cdot x + \mu_{DS})}$, where $x \sim N(0, 1)$	$\mu_{DS} = -6.8$ $\epsilon_{DS} = 0.288$	$\mu_{DS} = -6.18$ $\epsilon_{DS} = 0.18$	N/A
Mean total RMS DS	$\mathbb{E}(\sigma_{DS}) = 0.17\,\mu$s	$\mathbb{E}(\sigma_{DS}) = 0.65\,\mu$s	$\mathbb{E}(\sigma_{DS}) = 0.251\,\mu$s
$r_{DS} = \sigma_{\text{delays}}/\sigma_{DS}$	1.4	1.7	N/A
Distribution for path delays	–	–	$U(0, 1.2\,\mu\text{s})$
Lognormal shadowing standard deviation, σ_{SF}	8 dB	8 dB	NLOS: 10 dB LOS: 4 dB
Pathloss model (dB), d is in meters	$31.5 + 35\log_{10}(d)$	$34.5 + 35\log_{10}(d)$	NLOS: $34.53 + 38\log_{10}(d)$ LOS: $30.18 + 26\log_{10}(d)$

the MSs and for each of these drops, parameters describing the channel such as DS, AS, SF, AoAs, etc. are assumed to be fixed. For each new simulation drop, these parameters are randomly drawn according to the specified distributions that depend on the environment under invetigation. Furthermore, the MS position is also drawn randomly for each new drop. Since the model is antenna independent, for each simulation run the antenna patterns, geometries and orientations can be chosen arbitrary. Table 1 summarizes the SCM channel parameters used in each of the environments.

In addition to the 3-steps procedure as described above, the SCM offers four optional system simulation features for special cases (see Fig. 5).

- **Polarized arrays**: The cross-polarized model is included in additional to the vertical-polarized one assumed in the baseline model. Cross-polarized antenna arrays will most likely to be implemented on future handheld devices in order to guarantee the compact size of the devices.
- **Far scatterer clusters**: The far scatterer clusters represent bad-urban case where additional clusters are seen in the environment. These can be due to reflection or scattering caused by mountains, high-rise buildings, etc. The far scatterers tend to increase both the delay and angular spreads of the channel which can change the MIMO channel characteristics significantly. Note that this feature is limited to be used in the urban macrocell only.
- **Line-of-sight (LOS)**: The LOS modeling is based on the Ricean-K factor and is available for urban microcell only. By including the LOS path in the model, the average delay and angular spreads are reduced, which represent a highly correlated MIMO channel.
- **Urban canyon**: Urban canyon exists in dense urban areas where signals propagate between buildings which typically occur in both macrocells and over rooftop microcells. Under this environment, multipath arrive at the MS are usually from similar angles which give rise to narrow AS. Therefore, this tends to increase the correlation at the MS. This feature is available for urban macrocell and urban microcell.

Interested readers are referred to [32] and [68] for more comprehensive description and evaluation of the 3GPP/3GPP2 SCM.

3.2 ITU-R IMT-Advanced MIMO Channel Model (IMT-Adv MCM)

The Drafting Group Evaluation Channel Model (DG-EVAL Channel Model) was formed within the ITU-R in order to develop standard MIMO channel modeling approach for the evaluation of IMT-Advanced candidate radio interface technologies (RITs). The DG-EVAL Channel Model was established in May 2007 during the 22nd Meeting of ITU-R Working Party 8F (WP8F) in Kyoto, Japan. The work within the group was continued in January 2008 during the 1st Meeting of ITU-R WP5D in Geneva, Switzerland and was finalized in July 2008 during the 2nd Meeting of ITU-R WP5D in Dubai, United Arab Emirates. The IMT-Adv MCM covers all the required test environments (TEs) and scenarios as defined in the IMT-Advanced RITs Evaluation Guidelines (IMT.EVAL) [35] which can be summarized as below:

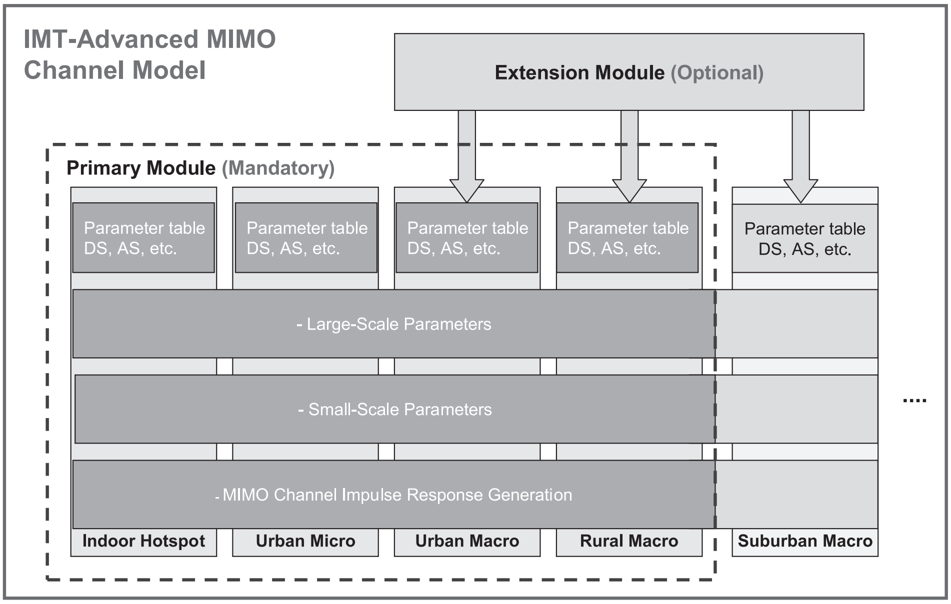

Fig. 6 The ITU-R IMT-Advanced MIMO channel model [35].

- **Base Coverage Urban TE**: Urban macrocell (UMa) scenario and suburban macrocell (SMa) scenario targeting on continuous coverage for pedestrian up to fast vehicular users. Note that SMa is defined as an optional scenario for evaluation within the WP5D.
- **Microcellular TE**: Urban microcell (UMi) scenario targeting on pedestrian and slow vehicular users in higher user density area.
- **Indoor TE**: Indoor hotspot (InH) scenario targeting on stationary and pedestrian in isolated cells.
- **High Speed TE**: Rural macrocell (RMa) scenario targeting on high-speed vehicular and trains.

The IMT-Adv MCM consists of a Primary Module (PM) and an Extension Module (EM) as illustrated in Fig. 6. The PM defines the mandatory channel model definition and parameter tables required for evaluation of IMT-Advanced candidate RITs in four mandatory scenarios i.e., UMa, UMi, InH and RMa. The EM is an optional feature available for UMa, RMa and SMa scenarios to cover cases beyond IMT-Advanced. In the rest of the paper, only the mandatory PM will be discussed.

The framework of the PM is based on the WINNER II channel model [64] which was developed within the European collaborate research project IST-WINNER. The PM is based upon the SCM methodology and is further extended to support system with larger bandwidths (i.e., up to 100 MHz) and different carrier frequencies (i.e., 2–6 GHz) in larger variety of different scenarios (i.e., from outdoor to indoor). The model parameters are determined from extensive wideband MIMO radio-channel measurement campaigns performed within IST-WINNER project and from results obtained in the literature. Within the PM, two models are defined, namely, the *generic model* and the *clustered delay line (CDL) model*. The generic model which is described

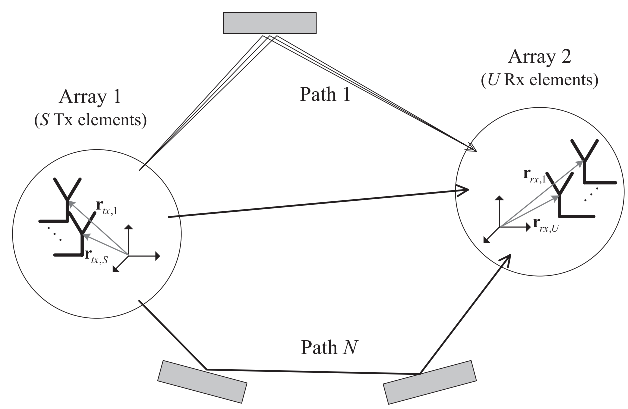

Fig. 7 The elements of the MIMO channel model as defined in the PM [35].

by one mathematical framework through different parameter sets will be used as the mandatory system-level model, while the CDL model is a reduced variability model with fixed parameter sets will only be used for calibration purposes.

Figure 7 illustrates the elements of the MIMO channel as defined in the PM. The MIMO channel transfer matrix is given by

$$\mathbf{H}(t;\tau) = \sum_{n=1}^{N} \mathbf{H}_n(t;\tau), \tag{4}$$

where t is time, τ is delay, N is the number of paths, and n is the path index. The channel between the TX antenna element s and RX antenna element u for path n is expressed by

$$H_{u,s,n}(t;\tau) = \sum_{m=1}^{M} \begin{bmatrix} F_{\mathrm{Rx},u,V}(\varphi_{n,m}) \\ F_{\mathrm{Rx},u,H}(\varphi_{n,m}) \end{bmatrix}^{T}$$

Table 2 The ITU-R IMT-Adv MCM channel model parameters for the generic model of PM [35].

Channel Scenario		InH		UMi			UMa		RMa		SMa	
		LOS	NLOS	LOS	NLOS	O-to-I	LOS	NLOS	LOS	NLOS	LOS	NLOS
Number of paths, N		15	19	12	19	12	12	20	11	10	15	14
Number of subpaths, M		20	20	20	20	20	20	20	20	20	20	20
Mean DS [ns]		20	39	65	129	240	93	365	32	37	59	74
Mean AS at BS [°]		40	42	16	26	58	14	26	8	9	59	75
Mean AS at MS [°]		42	59	56	69	18	65	74	33	33	30	45
Delay spread (DS),	μ	−7.70	−7.41	−7.19	−6.89	−6.62	−7.03	−6.44	−7.49	−7.43	−7.23	−7.12
$\log_{10}([s])$	σ	0.18	0.14	0.40	0.54	0.32	0.66	0.39	0.55	0.48	0.38	0.33
AoD spread (ASD),	μ	1.60	1.62	1.20	1.41	1.25	1.15	1.41	0.90	0.95	0.78	0.90
$\log_{10}([°])$	σ	0.18	0.25	0.43	0.17	0.42	0.28	0.28	0.38	0.45	0.12	0.36
AoA spread (ASA),	μ	1.62	1.77	1.75	1.84	1.76	1.81	1.87	1.52	1.52	1.48	1.65
$\log_{10}([°])$	σ	0.22	0.16	0.19	0.15	0.16	0.20	0.11	0.24	0.13	0.20	0.25
Shadow fading (SF), [dB]	σ	3	4	3	4	7	4	6	4	8	4	8
K-factor (K), [dB]	μ	7	N/A	9	N/A	N/A	9	N/A	7	N/A	9	N/A
	σ	4	N/A	5	N/A	N/A	3.5	N/A	4	N/A	7	N/A
Cross-correlation:												
σ_{ASD} vs. σ_{DS}		0.6	0.4	0.5	0	0.4	0.4	0.4	0	−0.4	0	0
σ_{ASA} vs. σ_{DS}		0.8	0	0.8	0.4	0.4	0.8	0.6	0	0	0.8	0.7
σ_{ASA} vs. σ_{SF}		−0.5	−0.4	−0.4	−0.4	0	−0.5	0	0	0	−0.5	0
σ_{ASD} vs. σ_{SF}		−0.4	0	−0.5	0	0.2	−0.5	−0.6	0	0.6	−0.5	−0.4
σ_{DS} vs. σ_{SF}		−0.8	−0.5	−0.4	−0.7	−0.5	−0.4	−0.4	−0.5	−0.5	−0.6	−0.4
σ_{ASD} vs. σ_{ASA}		0.4	0	0.4	0	0	0	0.4	0	0	0	0
ASD vs. K		0	N/A	−0.2	N/A	N/A	0	N/A	0	N/A	0	N/A
ASA vs. K		0	N/A	−0.3	N/A	N/A	0	N/A	0	N/A	−0.2	N/A
DS vs. K		−0.5	N/A	0.7	N/A	N/A	−0.4	N/A	0	N/A	0	N/A
SF vs. K		0.5	N/A	0.5	N/A	N/A	0	N/A	0	N/A	0	N/A
Delay distribution		Exponential										
AoD and AoA distribution		Laplacian		Wrapped Gaussian								
Delay scaling parameter, r_τ		3.6	3	3.2	3	2.2	2.5	2.3	3.8	1.7	2.4	1.5
XPR [dB]	μ	11	10	9	8	9	8	7	12	7	8	4
Cluster ASD		5	5	3	10	5	5	2	2	2	5	2
Cluster ASA		8	11	17	22	8	11	15	3	3	5	10
Per cluster shadowing standard deviation, ζ [dB]		6	3	3	3	4	3	3	3	3	3	3
Correlation distance [m]	DS	8	5	7	10	10	30	40	50	36	6	40
	ASD	7	3	8	10	11	18	50	25	30	15	30
	ASA	5	3	8	9	17	15	50	35	40	20	30
	SF	10	6	10	13	7	37	50	37	120	40	50
	K	4	N/A	15	N/A	N/A	12	N/A	40	N/A	10	N/A

$$
\begin{aligned}
&\times \begin{bmatrix} \alpha_{n,m,VV} & \alpha_{n,m,VH} \\ \alpha_{n,m,HV} & \alpha_{n,m,HH} \end{bmatrix} \begin{bmatrix} F_{\mathrm{Tx},s,V}(\phi_{n,m}) \\ F_{\mathrm{Tx},s,H}(\phi_{n,m}) \end{bmatrix} \\
&\times \exp\left(j2\pi\lambda_0^{-1}\left(\bar{\varphi}_{n,m}\cdot\bar{r}_{\mathrm{Rx},u}\right)\right) \\
&\times \exp\left(j2\pi\lambda_0^{-1}\left(\bar{\phi}_{n,m}\cdot\bar{r}_{\mathrm{Tx},s}\right)\right) \\
&\times \exp\left(j2\pi\nu_{n,m}t\right)\cdot\delta\left(\tau-\tau_{n,m}\right), \qquad (5)
\end{aligned}
$$

where $F_{\mathrm{Rx},u,V}$ and $F_{\mathrm{Rx},u,H}$ are the antenna element u field patterns for vertical and horizontal polarization, respectively, $\alpha_{n,m,VV}$ and $\alpha_{n,m,VH}$ are the complex gains of the vertical-to-vertical and vertical-to-horizontal polarizations of ray n, m, respectively, λ_0 is the wavelength of the carrier frequency, $\bar{\phi}_{n,m}$ and $\bar{\varphi}_{n,m}$ are the AoD and AoA unit vector, respectively, $\bar{r}_{\mathrm{Tx},s}$ and $\bar{r}_{\mathrm{Rx},u}$ are the location vectors of element s and u, respectively, and $\nu_{n,m}$ is the Doppler frequency component of ray n, m.

The generic model is a stochastic model with three levels of randomness [35]. Firstly, the LS parameters are drawn randomly from the tabulated distribution functions (see Table 2). These parameters are assumed to be constant over some large area of several wavelengths. Secondly, the SS parameters are drawn randomly according to the tabulated distribution functions and random LS parameters. Finally, by randomly selecting different initial phases, an infinite number of different realizations of the model can be generated. Similar to the approach used in the SCM, the drop concept will also be used by the generic model to simulate the time-evolution conditions. In general, the overall procedure for generating the channel coefficients based on the PM of the IMT-Adv MCM can be summarized in three stages as illustrated in Fig. 8. The first stage consists of two steps i.e., the propagation scenario selection, and the network layout and antenna configuration determination. In the second stage, both LS and SS parameters are defined. Finally, in the third stage, channel coefficients are computed. Note that, the PM channel model creation process is similar to the SCM one as described in Sect. 3.1. Table 2 summarizes the generic model channel parameters used in each of the TEs and scenarios. Here, the number of paths are fixed to different values for different scenarios, ranging from 10 to

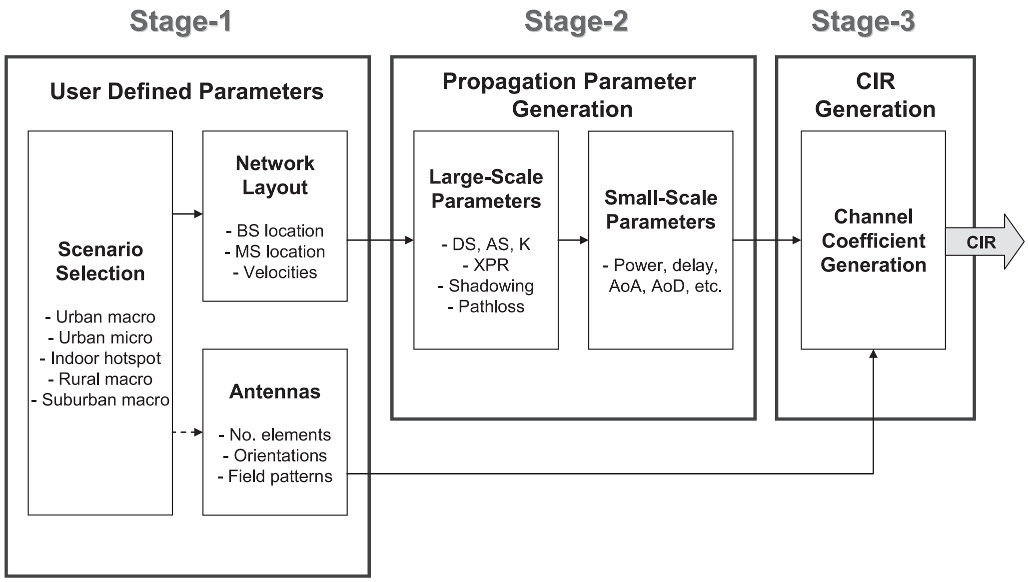

Fig. 8 The overview of the channel coefficients generation procedure based on the PM of the IMT-Adv MCM [35].

Table 3 The ITU-R IMT-Adv pathloss models [35].

Channel Scenario	Pathloss [dB]	SF Std [dB]	Default Values
InH LOS	$PL = 16.9\log_{10}(d) + 46.8 + 20\log_{10}(f_c/5.0)$	$\sigma = 3$	$3 < d < 100$ [m] $h_{\mathrm{BS}} = 3-6$ [m] $h_{\mathrm{MS}} = 1-2.5$ [m]
InH NLOS	$PL = 43.3\log_{10}(d) + 25.5 + 20\log_{10}(f_c/5.0)$	$\sigma = 4$	$10 < d < 150$ [m] $h_{\mathrm{BS}} = 3-6$ [m] $h_{\mathrm{MS}} = 1-2.5$ [m]
InH FAF (Optional)	For any of the above, add Floor Attenuation Factor (FAF) if the BS and MS are in different floors: $FAF = 20 + 6(n_f - 1)$ [dB]	$\sigma = 4$	n_f: number of floors between the BS and the MS ($n_f > 0$)
UMi LOS	$PL = 22\log_{10}(d) + 42 + 20\log_{10}(f_c/5.0)$ $PL = 40\log_{10}(d_1) + 9.2 - 18\log_{10}(h'_{\mathrm{BS}})$ $-18\log_{10}(h'_{\mathrm{MS}}) + 2\log_{10}(f_c/5.0)$	$\sigma = 3$ $\sigma = 3$	$10 < d_1 < d'_{\mathrm{BP}}$ [m] $d'_{\mathrm{BP}} < d_1 < 5000$ [m] $h_{\mathrm{BS}} = 10$, $h_{\mathrm{MS}} = 1.5$ [m] where $d'_{\mathrm{BP}} = 4h'_{\mathrm{BS}}h'_{\mathrm{MS}}f_c/c$, $c = 3\times10^8$ m/s $h'_{\mathrm{BS}} = h_{\mathrm{BS}} - 1$ and $h'_{\mathrm{MS}} = h_{\mathrm{MS}} - 1$
UMi NLOS	**Manhattan grid layout (optional)**: $PL = \min(PL(d_1, d_2), PL(d_2, d_1))$ where $PL(d_k, d_l) = PL_{\mathrm{LOS}}(d_k) + 20 - 12.5n_j$ $+10n_j\log_{10}(d_l) + 3\log_{10}(f_c/5.0)$, with $n_j = \max(2.8 - 0.0024d_k, 1.84)$, PL_{LOS} is the pathloss of UMi LOS, and $k, l \in \{1, 2\}$ **Hexagonal layout**: $PL = 36.7\log_{10}(d) + 40.9 + 26\log_{10}(f_c/5.0)$	$\sigma = 4$ $\sigma = 4$	$20 < d_1 + d_2 < 5000$ [m] $w/2 < \min(d_1, d_2)$ $w = 20$ [m] (street width) $h_{\mathrm{BS}} = 10$, $h_{\mathrm{MS}} = 1.5$ [m] where d_1 is the distance from the BS to the center of the perpendicular street, and d_2 is the distance from the MS along the perpendicular street. When $0 < \min(d_1, d_2) < w/2$, the LOS PL is applied. $10 < d < 2000$ [m] $h_{\mathrm{BS}} = 10$, $h_{\mathrm{MS}} = 1-2.5$ [m]
UMi O-to-I	$PL = PL_{\mathrm{b}} + PL_{\mathrm{tw}} + PL_{\mathrm{in}}$ **Manhattan grid layout (optional)**: $PL_{\mathrm{b}} = PL_{B1}(d_{\mathrm{out}} + d_{\mathrm{in}})$ $PL_{\mathrm{tw}} = 14 + 15(1 - \cos(\theta))^2$ $PL_{\mathrm{in}} = 0.5d_{\mathrm{in}}$ **Hexagonal layout**: $PL_{\mathrm{tw}} = 20$, other values remain the same.	$\sigma = 7$	$3 < d_{\mathrm{out}} + d_{\mathrm{in}} < 1000$ [m] $h_{\mathrm{BS}} = 10$, $h_{\mathrm{MS}} = 3(n_{Fl} - 1) + 1.5$ [m] where PL_{b}: basic pathloss, PL_{B1}: loss of UMi outdoor scenarios, PL_{tw}: loss through wall, PL_{in}: loss inside, d_{out}: distance from BS to wall next to MS, d_{in}: perpendicular distance from wall to MS, θ: angle between LOS to wall.

Table 4 (continued) The ITU-R IMT-Adv pathloss models [35].

Channel Scenario	Pathloss [dB]	SF Std [dB]	Default Values
UMa LOS	$PL = 22\log_{10}(d) + 42 + 20\log_{10}(f_c/5.0)$	$\sigma = 4$	$10 < d < d'_{BP}$ [m]
	$PL = 40\log_{10}(d_1) + 9.2 - 18\log_{10}(h'_{BS})$ $-18\log_{10}(h'_{MS}) + 2\log_{10}(f_c/5.0)$	$\sigma = 4$	$d'_{BP} < d < 5000$ [m] $h_{BS} = 25$, $h_{MS} = 1.5$ [m] (d'_{BP}, h_{BS} and h'_{MS} are defined in UMi LOS.)
UMa NLOS	$PL = 101.04 - 7.1\log_{10}(w) + 7.5\log_{10}(h)$ $-(24.37 - 3.7(h/h_{BS})^2)\log_{10}(h_{BS})$ $+(43.42 - 3.1\log_{10}(h_{BS}))(\log_{10}(d) - 3)$ $+20\log_{10}(f_c) - (3.2(\log_{10}(11.75h_{MS}))^2 - 4.97)$	$\sigma = 4$	$h = 20$ [m] (average building height) $w = 20$ [m] (street width) $h_{BS} = 25$, $h_{MS} = 1.5$ [m], The applicability ranges: [m] $5 < h < 50$, $5 < w < 50$, $10 < h_{BS} < 150$, $1 < h_{MS} < 10$, $50 < d < 5000$
RMa LOS	$PL = 20\log_{10}\left(\frac{4\pi(d)}{300/f_c}\right) + \min(0.03h^{1.72}, 10)\log_{10}(d)$ $-\min(0.044h^{1.72}, 14.77) + 0.002\log_{10}(h)d$	$\sigma = 4$	$10 < d < d_{BP}$ [m]
	$PL = 40\log_{10}(d) - 20\log_{10}(h_{BS}) - 20\log_{10}(h_{MS})$ $+5\log_{10}(f_c) + 11\log_{10}(h) - 7.1\log 10(w) - 2.45$	$\sigma = 6$	$d_{BP} < d < 10,000$ [m] $h_{BS} = 32$, $h_{MS} = 1.5$ [m] $w = 20$, $h = 5$ [m] where $d_{BP} = 2\pi h_{BS}h_{MS}f_c/c$ (The applicability ranges of h, w, h_{BS}, h_{MS} are same as in UMa NLOS)
RMa NLOS	$PL = 101.04 - 7.1\log_{10}(w) + 7.5\log_{10}(h)$ $-(24.37 - 3.7(h/h_{BS})^2)\log_{10}(h_{BS})$ $+(43.42 - 3.1\log_{10}(h_{BS}))(\log_{10}(d) - 3)$ $+20\log_{10}(f_c) - (3.2(\log_{10}(11.75h_{MS}))^2 - 4.97)$	$\sigma = 8$	$50 < d < 5000$ [m] $h_{BS} = 32$, $h_{MS} = 1.5$ [m] $w = 20$, $h = 5$ [m] (The applicability ranges of h, W, h_{BS}, h_{MS} are same as in UMa NLOS)
SMa LOS (Optional)	$PL = 20\log_{10}\left(\frac{4\pi(d)}{300/f_c}\right) + \min(0.03h^{1.72}, 10)\log_{10}(d)$ $-\min(0.044h^{1.72}, 14.77) + 0.002\log_{10}(h)d$	$\sigma = 4$	$30 < d < d_{BP}$ [m]
	$PL = 40\log_{10}(d) - 20\log_{10}(h_{BS}) - 20\log_{10}(h_{MS})$ $+5\log_{10}(f_c) + 11\log_{10}(h) - 7.1\log 10(w) - 2.45$	$\sigma = 6$	$d_{BP} < d < 5000$ [m] $h_{BS} = 32$, $h_{MS} = 1.5$ [m] $w = 20$, $h = 10$ [m] (The applicability ranges of h, w, h_{BS}, h_{MS} are same as in UMa NLOS. d_{BP} is defined in RMa LOS.)
SMa NLOS (Optional)	$PL = 101.04 - 7.1\log_{10}(w) + 7.5\log_{10}(h)$ $-(24.37 - 3.7(h/h_{BS})^2)\log_{10}(h_{BS})$ $+(43.42 - 3.1\log_{10}(h_{BS}))(\log_{10}(d) - 3)$ $+20\log_{10}(f_c) - (3.2(log_{10}(11.75h_{MS}))^2 - 4.97)$	$\sigma = 8$	$50 < d < 5000$ [m] $h_{BS} = 25$, $h_{MS} = 1.5$ [m] $w = 20$, $h = 10$ [m] (The applicability ranges of h, W, h_{BS}, h_{MS} are same as in UMa NLOS)

20 and each path consists of 20 fixed subpaths.

Tables 3 and 4 summarize the pathloss models for all the TEs and scenarios. In this table, distance d is in meters and center frequency f_c is in GHz. These models can be applied in the frequency range from 2–6 GHz and for different antenna heights. The RMa pathloss formula can also be applied to the desired frequency range around 800 MHz. Here, the shadow fading is assumed to be lognormal distributed and the standard deviation (Std) for each scenario is given in the table.

4. Performance Metrics Evaluation of SCM and IMT-Adv MCM

Two performance metrics often used to characterize the MIMO channel models are the *spatial multiplexing gain* and the *spatial diversity gain*. These two parameters have a crucial impact on the wireless communications system deploying MIMO techniques. For instance, for the same bandwidth, spatial multiplexing can offer a linear capacity increment proportional to the number of antennas at the BS and MS without additional power expenditure [69]. Note that, this can only be achieved when different data bits are transmitted via several independent spatial channels. On the other hand, spatial diversity utilizes two or more antennas to combat fading in order to improve the quality and reliability of a wireless link. The two most frequently used spatial diversity techniques in MIMO system are the receive diversity and the transmit diversity. The 3GPP/3GPP2 SCM has been widely used for the Beyond 3G/4G cellular system evaluation. However, the IMT-Adv MCM is a fairly new channel model and has not been well studied. Table 5 compares the similarities and differences of these two MIMO channel models.

In this section, the spatial multiplexing and spatial diversity gains of these channel models are evaluated for different environments (e.g., urban macro, suburban macro, and urban micro). The MIMO channel coefficients for both

Table 5 The 3GPP/3GPP2 SCM vs. ITU-R IMT-Adv MCM.

Parameters	3GPP/3GPP2 SCM	IMT-Adv MCM
Environments/scenarios	Urban Macro (NLOS)	Urban Macro (LOS & NLOS)
	Urban Micro (NLOS & LOS)	Urban Micro (LOS, NLOS & O-to-I)
	Suburban Macro (NLOS)	Suburban Macro (LOS & NLOS)
	–	Rural Macro (LOS & NLOS)
	–	Indoor Hotspot (LOS & NLOS)
Frequency range	2 GHz	2 – 6 GHz
Maximum bandwidth	5 MHz	100 MHz
Mobility	Up to 120 km/h	Up to 350 km/h
Number of paths, N	6	4 – 20
Number of subpaths per path, M	20	20
BS angle spread	5 – 19°	6 – 42°
MS angle spread	68°	30 – 74°
Delay spread	170 – 650 ns	20 – 365 ns
Shadow fading standard deviation	4 – 10 dB	1 – 1.8 dB
Correlation between LS parameters	No	Yes

models are generated using methods described in Sect. 3.1 and Sect. 3.2. The time-delay domain MIMO channel matrix can be expressed as follows

$$\mathbf{h}_{n,t,d} = (h_{u,s,n,t,d})_{U\times S}\,, \tag{6}$$

where U and S are the total number of antenna elements at the MS and BS, respectively, u and s are the index of MS and BS antenna elements, respectively, n is the index of delay paths, and t is the index of time-sample in the d-th drop. In this paper, we will consider a downlink system where a BS transmits to a MS. The same principle can be applied to uplink systems as well. By taking a discrete Fourier transform in the delay domain, the time-frequency domain MIMO channel matrix is given by

$$\mathbf{H}_{f,t,d} = \left(H_{u,s,f,t,d}\right)_{U\times S}\,, \tag{7}$$

where f is the index of the narrowband frequency bins. The channel frequency response are then normalized in order to obtain unity power. The average power over all samples P_f are calculated as follows

$$P_f = \frac{1}{USFTD}\sum_{f=1}^{F}\sum_{t=1}^{T}\sum_{d=1}^{D}\left\|\mathbf{H}_{f,t,d}\right\|_{\mathcal{F}}^{2}. \tag{8}$$

where $\|\cdot\|_{\mathcal{F}}$ denotes the Frobenius norm, F, T, and D are the total number of narrowband frequency bins, the total time-samples, and the total number of simulation drops, respectively. The normalized channel coefficients can be obtained by

$$\overline{H}_{f,t,d} = \frac{H_{f,t,d}}{P_f}, \tag{9}$$

where the normalized channel matrix is given by

$$\overline{\mathbf{H}}_{f,t,d} = \left(\overline{H}_{f,t,d}\right)_{U\times S}\,. \tag{10}$$

4.1 Spatial Multiplexing

For each $(U \times S)$ channel matrix $\mathbf{H}$ realization, the *narrowband capacity* $C^{\mathbf{NB}}$ can be computed as follows [20], [21]

$$C^{\mathrm{NB}} = \log_2\left[\det\left(\mathbf{I} + \frac{\rho}{S}\mathbf{H}^{\mathcal{H}}\mathbf{H}\right)\right], \tag{11}$$

where $\mathbf{I}$ is the identity matrix, and ρ is the average per-receiver-antenna signal-to-noise ratio (SNR). For wideband channels, the *wideband capacity* $C^{\mathbf{WB}}$ is computed by integrating over all frequencies and is given by [70]

$$C^{\mathrm{WB}} = \frac{1}{B}\int_B \log_2\det\left(\mathbf{I} + \frac{\rho}{S}\mathbf{H}^{\mathcal{H}}(f)\mathbf{H}(f)\right)df, \tag{12}$$

where $\mathbf{H}(f)$ is the wideband channel frequency response, and B is the channel bandwidth of interest. Using the normalized channel matrix obtained from (10), the wideband capacity for each channel realization under ρ SNR can be calculated in the frequency domain by computing the average over the frequency bins as follows

$$C_{t,d}^{\mathrm{WB}} = \lim_{F\to\infty}\frac{1}{F}\sum_{f=1}^{F}\log_2\left|\mathbf{I} + \frac{\rho}{S}\overline{\mathbf{H}}_{f,t,d}^{\mathcal{H}}\overline{\mathbf{H}}_{f,t,d}\right|. \tag{13}$$

From the wideband capacity samples $\{C_{t,d}^{\mathrm{WB}}\}$, the capacity cumulative distribution function (cdf) F_{Cap} is given by

$$F_{\mathrm{Cap}}(c) \triangleq \frac{1}{TD}\sum_{t=1}^{T}\sum_{d=1}^{D} I\left(C_{t,d}^{\mathrm{WB}} \le c\right), \tag{14}$$

where the outage capacity C_q can be obtained from F_{Cap} such that $F_{\mathrm{Cap}}(C_q) = q$. The wideband capacity for the 3GPP/3GPP2 SCM and the IMT-Adv MCM are evaluated in urban macro, suburban macro, and urban micro environments under LOS and NLOS scenarios. Figures 9–11 show the complementary cdf (ccdf) of the 1000 channel realizations in these environments with four antenna elements at both BS and MS with $\rho = 14$ dB. Table 6 summarizes the $C_{0.05}$, $C_{0.5}$, and $C_{0.95}$ outage capacity of both channel models in these four environments.

From the results, we can see that the outage capacity of the IMT-Adv MCM is less than the 3GPP/3GPP2 SCM except for the urban macro environment. This implies that, if the same space-time signal processing technique is being deployed in both channel models, the system will experience lower capacity in the IMT-Adv MCM. In particular, the reduction of the spatial multiplexing gain in the IMT-Adv MCM under the NLOS scenario could be due the presence of fewer dominant scatterers in the environment. This tends to increase the channel correlation and cause the loss of MIMO channel rank.

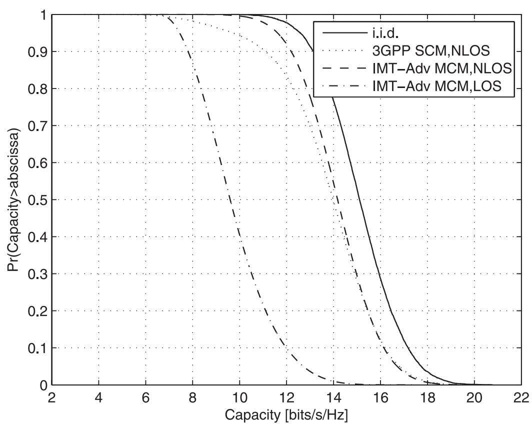

Fig. 9 The ccdf of the wideband capacity in urban macro environment with four antenna elements and $\rho = 14$ dB.

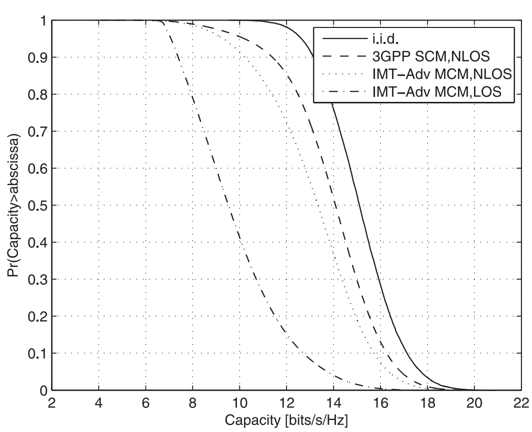

Fig. 10 The ccdf of the wideband capacity in suburban macro environment with four antenna elements and $\rho = 14$ dB.

4.2 Spatial Diversity

The spatial diversity gain of a MIMO channel is specified by the *eigenvalues*, which define the number of independently fading components and its associated power. The number of significant eigenvalues specifies the maximum degree of diversity and the principal eigenvalue specifies the maximum possible beamforming gain. The diversity order is defined by the number of decorrelated spatial branches available at the TX or RX [71] which depends on the SNR and the type of RX. In order to contribute to the effective diversity order, an eigenvalue has to be significant with respective to the noise level and the strongest eigenvalue (which depends on the dynamic range of the RX).

Using the normalized channel matrix obtained from (10), the eigenvalues for each channel realization $\lambda_{u,f,t,d}$ can be calculated through eigenvalue decomposition which are ordered in descending order as

$$\lambda_{1,f,t,d} \geq \lambda_{2,f,t,d} \geq \ldots \lambda_{U,f,t,d} \geq 0. \tag{15}$$

The eigenvalue cdf $F_{\mathrm{Div}}^{(u)}$ can be obtained from

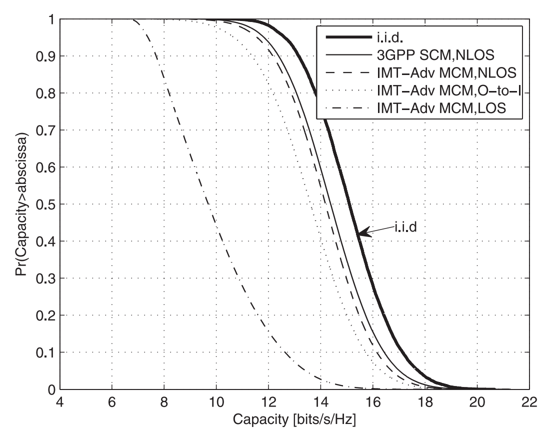

Fig. 11 The ccdf of the wideband capacity in urban micro environment with four antenna elements and $\rho = 14$ dB.

Table 6 The outage capacity of the 3GPP/3GPP2 SCM and the ITU-R IMT-Adv MCM.

Environments/scenarios	3GPP/3GPP2 SCM ($4 \times 4, \rho = 14$ dB)			IMT-Adv MCM ($4 \times 4, \rho = 14$ dB)		
	$C_{0.05}$	$C_{0.5}$	$C_{0.95}$	$C_{0.05}$	$C_{0.5}$	$C_{0.95}$
Urban macro LOS	–	–	–	7.4444	9.6001	12.7113
Urban macro NLOS	9.7130	13.9822	16.8070	11.6162	14.1740	16.7158
Urban micro LOS	10.5633	14.1624	16.9460	7.3768	9.6908	13.4272
Urban micro NLOS	11.8282	14.3828	17.0195	11.5602	11.1835	16.7211
Urban micro O-to-I	–	–	–	10.6796	13.6156	16.3326
Suburban macro LOS	–	–	–	7.0768	9.5202	13.7439
Suburban macro NLOS	10.1990	14.0846	16.8711	9.2947	13.3366	16.3602
Rural macro LOS	–	–	–	7.4829	9.7582	12.9047
Rural macro NLOS	–	–	–	9.1013	12.7466	15.8575
Indoor hotspot LOS	–	–	–	7.8480	10.4266	13.5620
Indoor hotspot NLOS	–	–	–	10.6864	13.6669	16.3880

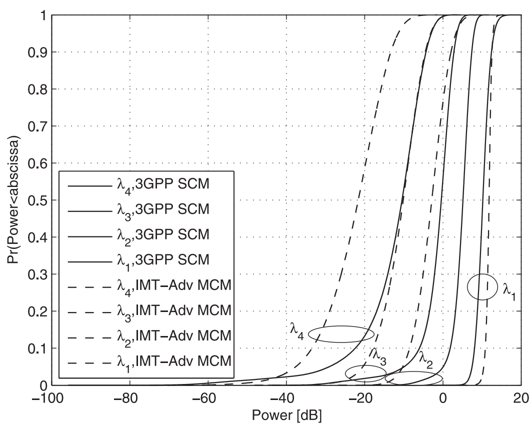

Fig. 12 The cdf of eigenvalues in urban macro environment with four antenna elements and $\rho = 14$ dB.

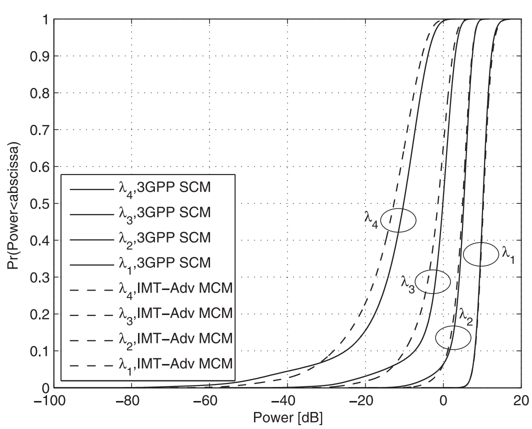

Fig. 13 The cdf of eigenvalues in suburban macro environment with four antenna elements and $\rho = 14$ dB.

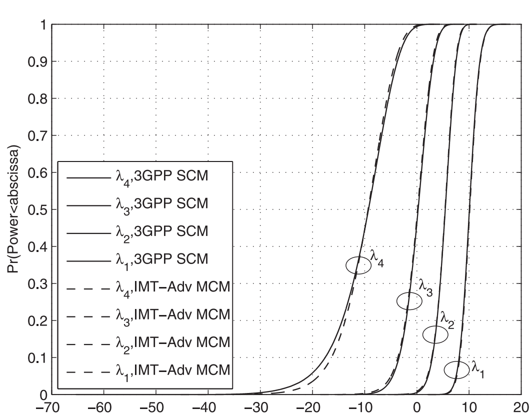

Fig. 14 The cdf of eigenvalues in urban micro environment with four antenna elements and $\rho = 14$ dB.

$$F^{(u)}_{\mathrm{Div}}(\lambda) \triangleq \frac{1}{TD}\sum_{t=1}^{T}\sum_{d=1}^{D} I\left(\overline{\lambda}_{u,t,d} \le \lambda\right), \tag{16}$$

where $\{\overline{\lambda}_{u,t,d}\}$ are the samples of the average eigenvalues given by

$$\overline{\lambda}_{u,t,d} = \frac{1}{F}\sum_{f=1}^{F}\lambda_{u,f,t,d}. \tag{17}$$

The spatial diversity metric $\lambda^{(u)}_q$ can be obtained from $F^{(u)}_{\mathrm{Div}}$ such that $F^{(u)}_{\mathrm{Div}}(\lambda^{(u)}_q) = q$. The spatial diversity for the 3GPP/3GPP2 SCM and the IMT-Adv MCM are evaluated in urban macro, suburban macro, and urban micro environments under NLOS scenario. Figures 12–14 show the cdf of the 1000 channel realizations in these environments with four antenna elements at both BS and MS with $\rho = 14$ dB. From the results, we can see that there are more significant eigenvalues in 3GPP/3GPP2 SCM as compare to the IMT-Adv MCM except in urban micro environment. This implies that higher diversity order is available in the SCM. Particularly in the urban macro environment, the strongest eigenvalue of the IMT-Adv MCM has much significant amount of energy as compare to the other eigenvalues. Therefore, for such an environment, technique such as beamforming is preferred than any spatial diversity techniques in order to exploit the multipath behavior of the channels.

5. Conclusion

In this paper, a survey of the propagation channel modeling works and the trend towards IMT-Advanced are presented. Firstly, various channel modeling approaches are discussed. This was followed by a review of some standard MIMO channel models used in 3G and B3G/4G cellular systems. In particular, the concepts that form the basis of the 3GPP/3GPP2 SCM and the IMT-Adv MCM are compared and described in detail. This includes the model mathematical framework, covered environments, and simulation procedure. Finally, two figure of merits that are important for MIMO systems, namely, spatial multiplexing and spatial diversity are used to compare the performance of the 3GPP/3GPP2 SCM and the IMT-Adv MCM, and their impacts on MIMO communication systems design are discussed.

References

[1] P.A. Bello, "Characterization of randomly time-variant linear channels," IEEE Trans. Commun. Syst., vol.CS-11, no.4, pp.360–393, Dec. 1963.
[2] R.H. Clarke, "A statistical theory of mobile-radio reception," Bell Syst. Tech. J., vol.47, no.1, pp.957–1000, July 1968.
[3] G. Turin, F.D. Clapp, T.L. Johnston, S.B. Fine, and D. Lavry, "A statistical model of urban multipath propagation," IEEE Trans. Veh. Technol., vol.VT-21, no.1, pp.1–9, Feb. 1972.
[4] W. Jakes, Microwave Mobile Communications, Wiley Interscience, New York, NY, 1974.
[5] T. Aulin, "Characteristics of a digital mobile radio channel," IEEE Trans. Veh. Technol., vol.VT-30, no.2, pp.45–53, May 1981.
[6] M. Hata, "Empirical formulas for propagation loss in land mobile radio service," IEEE Trans. Veh. Technol., vol.29, no.3, pp.317–325, Aug. 1980.
[7] W.C.Y. Lee, Mobile Communications Engineering, McGraw-Hill, New York, NY, 1982.
[8] F. Ikegami, S. Yoshida, T. Takeuchi, and M. Umehira, "Propagation

factors controlling mean field strength on urban streets," IEEE Trans. Antennas Propag., vol.32, no.8, pp.822–829, Aug. 1984.

[9] J. Walfish and H.L. Bertoni, "A theoretical model of UHF propagation in urban environments," IEEE Trans. Antennas Propag., vol.36, no.12, pp.1788–1796, Dec. 1988.

[10] E. Damosso, Digital Mobile Radio: COST 231 View on the Evolution Towards 3rd Generation Systems, Commission of the European Union, Final Report of the COST 231 Project, 1998.

[11] M. Failli, Digital Land Mobile Radio Communications COST 207, Commission of the European Union, Final Report of the COST 207 Project, 1989.

[12] Guidelines for Evaluation of Radio Transmission Technologies for IMT-2000, ITU Std. Recommendation ITU-R M.1225, 1997.

[13] R.B. Ertel, P. Cardieri, K.W. Sowerby, T.S. Rappaport, and J.H. Reed, "Overview of spatial channel models for antenna array communication systems," IEEE Pers. Commun. Mag., vol.5, no.1, pp.10–12, Feb. 1998.

[14] U. Martin, J. Fuhl, I. Gaspard, M. Haardt, A. Kuchar, C. Math, A.F. Molisch, and R. Thoma, "Model scenarios for direction-selective adaptive antennas in cellular mobile communication systems — Scanning the literature," Wirel. Pers. Commun., vol.11, no.1, pp.109–129, Oct. 1999.

[15] U. Martin, "Spatio-temporal radio channel characteristics in urban macrocells," IEE Proc. Radar, Sonar and Navigation, vol.145, no.1, pp.42–49, Feb. 1998.

[16] K. Kalliola and P. Vainikainen, "Dynamic wideband measurement of mobile radio channel with adaptive antennas," Proc. IEEE Semi-Annual Veh. Technol. Conf., vol.1, pp.21–25, Ottawa, Canada, May 1998.

[17] K.I. Pedersen, P. Mogensen, and B.H. Fleury, "A stochastic model of the temporal and azimuthal dispersion seen at the base s tation in outdoor propagation environments," IEEE Trans. Veh. Technol., vol.49, no.2, pp.437–447, March 2000.

[18] J.H. Winters, "On the capacity of radio communication systems with diversity in Rayleigh fading environment," IEEE J. Sel. Areas Commun., vol.5, no.5, pp.871–878, June 1987.

[19] G.J. Foschini, "Layered space-time architecture for wireless communication in a fading environment when using multi-element antennas," Bell Labs Tech. J., vol.1, no.2, pp.41–59, 1996.

[20] G.J. Foschini and M.J. Gans, "On limits of wireless communications in a fading environment when using multiple antennas," Wirel. Pers. Commun., vol.6, no.3, pp.311–335, March 1998.

[21] İ.E. Telatar, "Capacity of multi-antenna Gaussian channels," European Trans. Telecommun., vol.10, no.6, pp.585–595, Nov./Dec. 1999.

[22] M. Steinbauer, A.F. Molisch, and E. Bonek, "The double-directional radio channel," IEEE Antennas Propag. Mag., vol.43, no.4, pp.51–63, Aug. 2001.

[23] J. Laurila, K. Kalliola, M. Toeltsch, K. Hugl, P. Vainikainen, and E. Bonek, "Wide-band 3-D characterization of mobile radio channels in urban environment," IEEE Trans. Antennas Propag., vol.50, no.2, pp.233–243, Feb. 2002.

[24] M. Toeltsch, J. Laurila, K. Kalliola, A.F. Molisch, P. Vainikainen, and E. Bonek, "Statistical characterization of urban spatial radio channels," IEEE J. Sel. Areas Commun., vol.20, no.3, pp.539–549, April 2002.

[25] J.P. Kermoal, L. Schumacher, K.I. Pedersen, P.E. Mogensen, and F. Frederiksen, "A stochastic MIMO radio channel model with experimental validation," IEEE J. Sel. Areas Commun., vol.20, no.6, pp.1211–1226, Aug. 2002.

[26] K. Kalliola, H. Laitinen, P. Vainikainen, M. Toeltsch, J. Laurila, and E. Bonek, "3-D double-directional radio channel characterization for urban macrocellular applications," IEEE Trans. Antennas Propag., vol.51, no.11, pp.3122–3133, Nov. 2003.

[27] H. Xu, D. Chizhik, H. Huang, and R. Valenzuela, "A generalized space-time multiple input multiple output (MIMO) channel model," IEEE Trans. Wireless Commun., vol.3, no.4, pp.966–975, May 2004.

[28] W. Weichselberger, M. Herdin, H. Ozcelik, and E. Bonek, "A stochastic MIMO channel model with joint correlation of both link ends," IEEE Trans. Wireless Commun., vol.5, no.1, pp.90–100, Jan. 2006.

[29] A.F. Molisch, H. Asplund, R. Heddergott, M. Steinbauer, and T. Zwick, "The COST259 directional channel model — Part I: Overview and methodology," IEEE Trans. Wireless Commun., vol.5, no.12, pp.3421–3433, Dec. 2006.

[30] H. Asplund, A.A. Glazunov, A.F. Molisch, K.I. Pedersen, and M. Steinbauer, "The COST259 directional channel model — Part II: Macrocells," IEEE Trans. Wireless Commun., vol.5, no.12, pp.3434–3450, Dec. 2006.

[31] N. Costa and S. Haykin, "Novel wideband MIMO channel model and experimental validation," IEEE Trans. Antennas Propag., vol.56, no.2, pp.550–562, Feb. 2008.

[32] Spatial channel model for Multiple Input Multiple Output (MIMO) simulations (Release 7.0), 3rd Generation Partnership Project, Technical Specification Group Radio Access Network, 3GPP TR 25.996 V7.0.0, June 2007.

[33] WiMAX Forum Mobile Release 1.0 Channel Model, WiMAX Forum Std., June 2008.

[34] V. Erceg, et al., TGn Channel Models, IEEE P802.11 Wireless LANs Std., IEEE 802.11-03/940r4, May 2004.

[35] Draft New Report, "Guidelines for Evaluation of Radio Interface Technologies for IMT-Advanced," ITU Std. Document 5D/TEMP/90R1-E, July 2008.

[36] B.H. Fleury and P.E. Leuthold, "Radiowave propagation in mobile communications: An overview of European research," IEEE Commun. Mag., vol.34, no.2, pp.70–81, Feb. 1996.

[37] S.R. Saunders, Antennas and Propagation for Wireless Communication Systems, 1st ed., John Wiley & Sons, West Sussex, UK, 1999.

[38] T.S. Rappaport, Wireless Communications: Principles and Practice, 2nd ed., Prentice-Hall PTR, New Jersey, 2002.

[39] J.B. Andersen, T.S. Rappaport, and S. Yoshida, "Propagation measurements and models for wireless communications channels," IEEE Commun. Mag., vol.33, no.1, pp.42–49, Jan. 1995.

[40] W. Zhang, "Wide-band propagation model for cellular mobile radio communications," IEEE Trans. Antennas Propag., vol.45, no.11, pp.1669–1678, Nov. 1997.

[41] H.L. Bertoni, Radio Propagation for Modern Wireless Systems, Prentice-Hall, New Jersey, USA, 2000.

[42] T.S. Rappaport and S. Sandhu, "Radio-wave propagation for emerging wireless personal-communication systems," IEEE Antennas Propag. Mag., vol.36, no.5, pp.14–24, Oct. 1994.

[43] M.C. Lawton and J.P. McGeehan, "The application of a deterministic ray launching algorithm for the prediction of radio channel characteristics in small cell environments," IEEE Trans. Veh. Technol., vol.43, no.4, pp.955–969, Nov. 1994.

[44] M.F. Catedra, J. Perez, F.S. Adana, and O. Gutierrez, "Efficient ray-tracing techniques for three-dimensional analyses of propagation in mobile communications: Application to picocell and microcell scenarios," IEEE Antennas Propag. Mag., vol.40, no.2, pp.15–28, April 1998.

[45] G. Liang and H.L. Bertoni, "A new approach to 3-D ray tracing for propagation prediction in cities," IEEE Trans. Antennas Propag., vol.46, no.6, pp.853–863, June 1998.

[46] G.E. Athanasiadou, A.R. Nix, and J.P. McGeehan, "A microcellular ray-tracing propagation model and evaluation of its narrow-band and wide-band predictions," IEEE J. Sel. Areas Commun., vol.18, no.3, pp.322–335, March 2000.

[47] G.E. Athanasiadou and A.R. Nix, "Investigation into the sensitivity of the power predictions of a microcellular ray tracing propagation model," IEEE Trans. Veh. Technol., vol.49, no.4, pp.1140–1151, July 2000.

[48] K. Rizk, J.F. Wagen, and F. Gardiol, "Influence of database accuracy on two-dimensional ray-tracing-based predictions in urban micro-

cells," IEEE Trans. Veh. Technol., vol.49, no.2, pp.631–642, March 2000.
[49] M. Patzold, A. Szczepanski, and N. Youssef, "Methods for modeling of specified and measured multipath power-delay profiles," IEEE Trans. Veh. Technol., vol.51, no.5, pp.978–988, Sept. 2002.
[50] D. Gesbert, H. Bolcskei, D.A. Gore, and A.J. Paulraj, "Outdoor MIMO wireless channels: Models and performance prediction," IEEE Trans. Commun., vol.50, no.12, pp.1926–1934, Dec. 2002.
[51] A. Domazetovic, L.J. Greenstein, N.B. Mandayam, and I. Seskar, "Propagation models for short-range wireless channels with predictable path geometries," IEEE Trans. Commun., vol.53, no.7, pp.1123–1126, July 2005.
[52] K.H. Ng, E.K. Tameh, A. Doufexi, M. Hunukumbure, and A.R. Nix, "Efficient multielement ray tracing with site-specific comparisons using measured MIMO channel data," IEEE Trans. Veh. Technol., vol.56, no.3, pp.1019–1032, May 2007.
[53] Z. Wang, E.K. Tameh, and A.R. Nix, "Joint shadowing process in urban peer-to-peer radio channels," IEEE Trans. Veh. Technol., vol.57, no.1, pp.52–64, Jan. 2008.
[54] V. Pérez and J. Jiménez, "Final propagation model," Tech. Rep. CoDiT Deliverable Number R2020/TDE/PS/DS/P/040/al, June 1994.
[55] R. Gollreiter, "Channel models," Tech. Rep. ATDMA Deliverable Number R2084/ESG/CC3/DS/P/029/bl, May 1994.
[56] J. Fuhl, A.F. Molisch, and E. Bonek, "Unified channel model for mobile radio systems with smart antennas," Proc. Inst. Electr. Eng. Radar, Sonar Navigat., vol.145, no.1, pp.32–41, Feb. 1998.
[57] J.J. Blanz and P. Jung, "A flexibly configurable spatial model for mobile radio channels," IEEE Trans. Commun., vol.46, no.3, pp.367–371, March 1998.
[58] O. Nørklit and J.B. Andersen, "Diffuse channel model and experimental results for array antennas in mobile environments," IEEE Trans. Antennas Propag., vol.46, no.6, pp.834–840, June 1998.
[59] A. Abdi and M. Kaveh, "A space–time correlation model for multielement antenna systems in mobile fading channels," IEEE J. Sel. Areas Commun., vol.20, no.3, pp.550–560, April 2002.
[60] P. Petrus, J.H. Reed, and T.S. Rappaport, "Geometrical-based statistical macrocell channel model for mobile environments," IEEE Trans. Commun., vol.50, no.3, pp.495–502, March 2002.
[61] C. Oestges, V. Erceg, and A.J. Paulraj, "A physical scattering model for MIMO macrocellular broadband wireless channels," IEEE J. Sel. Areas Commun., vol.21, no.5, pp.721–729, June 2003.
[62] D. Chizhik, G.J. Foschini, and R.A. Valenzuela, "Capacities of multi-element transmit and receive antennas: Correlations and keyholes," IET Electronics Letters, vol.36, no.13, pp.1099–1100, June 2000.
[63] D. Chizhik, G.J. Foschini, M.J. Gans, and R.A. Valenzuela, "Keyholes, correlations, and capacities of multielement transmit andreceive antennas," IEEE Trans. Wireless Commun., vol.1, no.2, pp.361–368, April 2002.
[64] P. Kyosti and et al., "WINNER II channel models," IST, Tech. Rep. IST-4-027756 WINNER II D1.1.2 V1.2, Sept. 2007.
[65] L.M. Correia, Mobile Broadband Multimedia Networks: Techniques, Models and Tools for 4G, Academic Press, Oxford, UK, 2006.
[66] Spatial channel model for Multiple Input Multiple Output (MIMO) simulations (Release 6.1), 3rd Generation Partnership Project, Technical Specification Group Radio Access Network, 3GPP TR 25.996 V6.1.0, Sept. 2003.
[67] D.S. Baum, J. Hansen, J. Salo, G.D. Galdo, M. Milojevic, and P. Kyosti, "An interim channel model for beyond-3G systems: Extending the 3GPP spatial channel model (SCM)," Proc. IEEE Semi-Annual Veh. Technol. Conf., vol.5, pp.3132–3136, Stockholm, Sweden, June 2005.
[68] G. Calcev, D. Chizhik, B. Goransson, S. Howard, H. Huang, A. Kogiantis, A.F. Molisch, A.L. Moustakas, D. Reed, and H. Xu, "A wideband spatial channel model for system-wide simulations," IEEE Trans. Veh. Technol., vol.56, no.2, pp.389–403, March 2007.
[69] A.J. Paulraj, D.A. Gore, R.U. Nabar, and H. Bolcskei, "An overview of MIMO communications-a key to gigabit wireless," Proc. IEEE, vol.92, no.2, pp.198–218, Feb. 2004.
[70] A.F. Molisch, M. Steinbauer, M. Toeltsch, E. Bonek, and R.S. Thoma, "A wideband spatial channel model for system-wide simulations," IEEE J. Sel. Areas Commun., vol.20, no.3, pp.561–569, April 2002.
[71] D. Gesbert, M. Shafi, D. shan Shiu, P.J. Smith, and A. Naguib, "From theory to practice: An overview of MIMO space-time coded wireless systems," IEEE J. Sel. Areas Commun., vol.21, no.3, pp.281–302, April 2003.

Chia-Chin Chong received the B.Eng. degree with first class honors from The University of Manchester, Manchester, U.K., and the Ph.D. degree from The University of Edinburgh, Edinburgh, U.K., both in electronics and electrical engineering, in 2000 and 2003, respectively. From January 2004 to September 2005, she was with Samsung Advanced Institute of Technology, Suwon, South Korea. Since October 2005, she has been with DOCOMO Communications Laboratories USA, Inc., Palo Alto, CA. She has done research in the areas of MIMO propagation channel measurements and modeling, UWB systems, ranging and localization techniques, and cooperative relaying. Dr. Chong received numerous awards including the IEE Prize in 1999, Joseph Higham Prize and GEC-Marconi Prize in 2000, IEE Vodafone Research Award in 2001, Richard Brown Prize in 2002, IEEE International Conference on Ultra-Wideband (ICUWB) Best Paper Award, DoCoMo USA Labs President Award and The Outstanding Young Malaysian Award all in 2006, as well as URSI Young Scientist Award and DOCOMO USA Labs President Award in 2008. She has served as Guest Editor for Special Issues in the EURASIP Journal on Wireless Communications and Networking (JWCN) and the EURASIP Journal on Applied Signal Processing. Currently, she serves as an Editor for the IEEE Transactions on Wireless Communications and the EURASIP JWCN. She has served on the Technical Program Committee (TPC) of various international conferences, the TPC Co-Chair for the Broadband Wireless Access Symposium of the IEEE ICCCN 2007, the TPC Co-Chair for the Wireless Communications Symposium of the IEEE ICC 2008, the Publicity Co-Chair for the IEEE PIMRC 2008, the Sponsorship Chair for CrownCom 2008, and the Tutorial Chair for IEEE ICCCN 2009. Dr. Chong is a Senior Member of the IEEE.

Fujio Watanabe received B.Eng., M.Eng., and Ph.D. degrees from the University of Electro-Communications, Tokyo, Japan, in 1993, 1995, and 1998, respectively. From 1994 to 1995 he was a government scholarship student visiting the Department of Electrical and Electronic Engineering, University of Adelaide, Australia. From 1998 to 2001, he worked at Nokia Research Center, Helsinki, Finland, where he worked for WLAN and Bluetooth systems. Since April 2001, he has been working at DOCOMO Communications Laboratories USA, Inc. His current research interests include, seamless communications, wireless security, 4G cellular systems and wireless broadband systems including UWB and WiMAX. He is also actively involved in IEEE 802 standardization. Dr. Watanabe is a Member of the IEEE.

Koshiro Kitao was born in Tottori, Japan, in 1971. He received B.S. and M.S. degrees from Tottori University, Tottori, Japan in 1994 and 1996, respectively. He joined the Wireless Systems Laboratories, Nippon Telegraph and Telephone Corporation (NTT), Kanagawa, Japan, in 1996. Since then, he has been engaged in the research and development of radio propagation for mobile communications. He is now Assistant Manager of the Radio Access Network Development Department, NTT DOCOMO, INC., Kanagawa, Japan. Mr. Kitao is a Member of the IEEE.

Tetsuro Imai was born in Tochigi, Japan, in 1967. He received his B.S. and Ph.D. degrees from Tohoku University, Japan, in 1991 and 2002, respectively. He joined the Wireless System Laboratories of Nippon Telegraph and Telephone Corporation (NTT), Kanagawa, Japan, in 1991. Since then, he has been engaged in the research and development of radio propagation, antenna systems and system design for mobile communications. He is now Manager of the Radio Access Network Development Department, NTT DOCOMO, INC., Kanagawa, Japan. He received the IEICE Young Researcher's Award in 1998 and the IEICE Best Paper Award in 2006. Dr. Imai is a Member of the IEEE.

Hiroshi Inamura received B.S. and M.S. degrees in Keio University, Japan. He joined NTT in 1990 and since 1999, he has been working for NTT DOCOMO, Inc. He joined DOCOMO Communications Laboratories USA, Inc. in 2006. His research interests are in the area of networking including transport protocol issues and their solutions for wireless and distributed systems. He participated in the IETF and OMA international standardization activities for mobile multimedia system and protocol standardization. He received an achievement award from the Information Processing Society of Japan for his contribution to the standardization of mobile multimedia protocol in 2004. He is a Member of IPSJ and ACM.